

## Studies of the flickering in cataclysmic variables

### VI. The location of the flickering light source in HT Cassiopeiae, V2051 Ophiuchi, IP Pegasi and UX Ursae Majoris

A. Bruch

Laboratório Nacional de Astrofísica, CP 21, 37500–000 Itajubá – MG, Brazil (albert@lna.br)

Received 21 December 1999 / Accepted 9 May 2000

**Abstract.** The scatter in the light curves of four eclipsing cataclysmic variables (CVs) is analyzed in order to find constraints for the location of the flickering light source in these systems. In all cases the “scatter curves” contain well defined eclipses which begin and end exactly at the phases of eclipse ingress and egress of individual system components: In HT Cas, V2051 Oph and UX Uma the scatter eclipse coincides with the white dwarf eclipse, in IP Peg with the hot spot eclipse. Moreover, in V2051 Oph, IP Peg and UX Uma the scatter is enhanced during phases of visibility of the hot spot. Together with similar results from earlier investigations these findings leave little doubt that the flickering in CVs can originate in two regions: the innermost accretions disk with the boundary layer and the white dwarf surface, and the region of impact of the stream of transferred matter from the secondary star upon the accretion disk. Two different techniques (termed ‘single’ and ‘ensemble’ method) to measure the scatter curves of CVs are advocated in the literature. A critical comparison of these techniques is performed. It is found that the ‘ensemble’ method yields reasonable results only under specific circumstances.

**Key words:** stars: variables: general – stars: binaries: eclipsing – stars: novae, cataclysmic variables – stars: individual: HT Cas – V2051 Oph, IP Peg, UX Uma

#### 1. Introduction

Cataclysmic variables are known to be interacting binary stars in which a Roche-lobe filling late type star (the secondary) loses mass to a white dwarf primary. In most of these systems the dominant light source at optical and ultraviolet wavelengths is an accretion disk formed around the white dwarf by matter transferred from the secondary star.

One of the most characteristic observational properties of all cataclysmic variables are stochastic brightness variations known as flickering, occurring on time scales of seconds and minutes with amplitudes ranging from a few dozen millimagnitudes up to more than an entire magnitude, depending on the subtype of the CV, the photometric state, and the individual system. Flickering is observed in almost all photometric states of CVs,

except during outbursts of classical and recurrent novae when only the optically thick expanding envelope around the system is visible, and during extreme low states of some stars when mass transfer from the secondary star is probably suspended and the accretion disk has vanished.

Although flickering is so typical for CVs it is not restricted to this kind of stars. It may rather be regarded as a fingerprint of systems with mass accretion via an accretion disk onto a central body. For example, several symbiotic stars (albeit only a minority!) exhibit flickering with characteristics very similar to those observed in CVs (Dobrzycka et al. 1996). Flickering is also doubtlessly present in low-mass x-ray binaries, although due to a lack of optical high speed photometry it is by far not as well documented in these systems as in CVs. An exception is Sco X-1 (see e.g. Hiltner & Mook 1967, Sandage et al. 1969 Robinson & Warner 1972, and Augusteijn et al. 1992). Herbst & Shevchenko (1999) have recently explained the irregular variations observed in UX Ori stars (i.e. early type T Tau stars with irregular variations on comparatively long time scales; for a more complete definition, see Herbst et al. 1994) as due to luminosity variations caused by unsteady accretion of matter onto the central star out of the surrounding disk. The longer time scales involved in these cases are naturally explained by the larger dimensions of the central bodies. A study of the irregular variations of AGNs along these guidelines may also be rewarding.

Whereas the assumption that flickering is intimately related to mass transfer in binary systems or mass accretion onto a central body (be it a single object or a component of a binary) is certainly well justified the nature of the underlying physical mechanism is by no means clear. It is even doubtful that a single mechanism can be pinpointed. The fact that flickering occurs in all CVs independent of whether they have well developed accretion disks as the non-magnetic systems, truncated disks as the intermediate polars, or no disks at all as the AM Her stars immediately suggests that more than one mechanism must be involved. This is supported by the differences of the statistical properties of the flickering in magnetic and non-magnetic CVs found in a comprehensive wavelet analysis of the flickering in numerous systems performed by Fritz & Bruch (1998). Moreover, Bruch (1996) and Bruch et al. (2000) have shown that in

the dwarf novae Z Cha and V893 Sco, respectively, a part of the short time scale flickering originates in the hot spot while the rest comes from the central parts of the accretion disk and/or the white dwarf. Localizing the flickering within a CV obviously constrains possible mechanisms. Therefore, in this study the location of the flickering light source is determined for several more systems.

This can best be done in eclipsing CVs by quantifying the random variations due to flickering in an ensemble of light curves as a function of the orbital phase (i.e. by measuring the scatter curve). During phases when the flickering light source is best visible the scatter of the brightness measurements in high-speed photometry within a small phase interval or with respect to the light curve averaged over many cycles should on the mean be enhanced while it should become small when the flickering light source is invisible (e.g. eclipsed).

This technique was first applied to the nova-like variable RW Tri by Horne & Stiening (1985). Later, Bruch (1996) developed a somewhat different technique and applied it to Z Cha. Similar studies were performed for HT Cas (Welsh & Wood 1995, Welsh et al. 1996), V893 Sco (Bruch et al. 2000), and again for RW Tri (Bennie et al. 1996). In this contribution the location of the flickering light source will be studied in four systems: HT Cas (a SU UMa type dwarf nova), V2051 Oph (a dwarf nova of no well established sub-type), IP Peg (a U Gem type dwarf nova) and UX UMa (a nova-like variable). With the exception of HT Cas none of them has been subjected to a corresponding study before.

Concerning the details to calculate the scatter curve two schools exist, called ‘single’ and ‘ensemble’ by Welsh et al. (1996). They will be compared to each other in Sect. 2 before the observational material on which the present study is based is presented in Sect. 3 and the ‘single’ method is applied to the data in Sect. 4. Finally, Sect. 5 contains a summary of the principal conclusions of this study.

## 2. Comparison of methods

Two different approaches to measure the scatter curve are described in the literature. The basic difference between the ‘single’ method described by Bruch (1996) and used successfully in the present study as well as by Bruch et al. (2000), and the ‘ensemble’ method first introduced by Horne & Stiening (1985) and later adopted by Welsh & Wood (1995) and Bennie et al. (1996), is as follows: In the first case the scatter is determined as a function of phase for each light curve of a given system individually. The difference between a smoothed light curve and the original one is taken to define the scatter. The average of many individual curves of this kind then constitutes the mean scatter curve. In the second case the scatter is defined by the deviation of the individual light curves at a given phase from the mean light curve (after trying to account for long term variations). Thus, the final scatter curve resulting from the ‘single’ method is the mean of the scatter, whereas in the ‘ensemble’ method it is the scatter around the mean. These are different things!

Welsh et al. (1996) compare the two methods qualitatively. However, a more rigorous comparison has never been made. Moreover, the ‘ensemble’ method is only described briefly in the references cited above. Therefore, before embarking on the main objective of the present study – the determination of the location of the flickering light source in four systems – a more thorough assessment of the basis of the ‘ensemble’ method and its relationship to the ‘single’ method is performed in this section.

### 2.1. The ‘ensemble’ method

The ‘ensemble’ method was introduced by Horne & Stiening (1985) who applied it to the nova-like variable RW Tri. In a quite straight forward way they define the rms-light curve as the root-mean-squared deviation between the individual light curves and their mean light curve as a function of phase. Horne & Stiening (1985) found the scatter to drop sharply in a small phase interval around eclipse centre and concluded “that the flickering light source is more compact than the steady disc light” and “that the flickering distribution is approximately centred on the disc”.

The simple approach of Horne & Stiening (1985) furnished sensible results because they made sure that all of their light curves were observed within a short interval of just four days and that the object of their study, RW Tri, is a UX UMa type nova-like variable and thus a member of the most stable class of CVs. Both points together minimize the importance of long term variations. Thus, the mean light curve is stable at all orbital phases.

This was different in the case of the study of HT Cas by Welsh & Wood (1995). They used the ‘ensemble’ method to calculate the scatter curve based on light curves which were collected over a time span of several years at different telescopes. Moreover, as a SU UMa type dwarf nova HT Cas is by far not as stable as RW Tri. These systems do not only exhibit flickering but also often much stronger long term variations and variations on orbital time scales than nova-like variables. Furthermore, there is no guarantee that those variations which are not attributable to flickering influence the entire light curve in the same way. On the contrary, there is ample evidence for variations in such stars which affect only a part of the orbit, e.g. variable hump amplitudes, appearance and disappearance of intermediate humps, or variations of the eclipse depth. Such effects have to be accounted for before the scatter curve of the flickering can be calculated from the differences between the individual and the mean light curves.

Moreover, Welsh & Wood (1995) introduced a bias into their analysis of the HT Cas light curves. They find that the mid-eclipse flux is variable and attribute it to long term secular trends. They remove this effect by applying “a small additive constant to each curve so that the mean flux at mid-eclipse remained constant”. This procedure is problematic because by *definition* it reduces the scatter of the individual light curves around the mean during eclipse minimum (and even minimizes

it if the flickering during eclipse is not stronger than at other phases).

In order to assess if this bias is serious or insignificant the method of Welsh & Wood (1995) was applied to the data of HT Cas used in this paper (see Sect. 3), assuming that the long-term behaviour of the system is not altogether different in the data set of Welsh & Wood (1995) and the present one. Since the light curves available here are only expressed in count rates (as opposed to fluxes) they were normalized to the mean out-of-eclipse brightness in order to put them onto a comparable scale. Thus, long-term brightness variations are assumed not to exist, leading to a lower limit of the scatter. Due to strongly variable eclipse depths (with respect to the out-of-eclipse light level) of HT Cas the resulting scatter curve has a *maximum* during eclipse phases if no correction is applied to the light curves. It turns into a very deep minimum if the data are treated in the same way as Welsh & Wood (1995) did.

Thus, the bias is potentially quite serious. The minimum in the scatter curve of Welsh & Wood (1995) at the eclipse phase is therefore in the first place caused by the method. Even if the flickering really is eclipsed at these phases – as shown in Sect. 4.1 – this is not the primary cause for the minimum found by Welsh & Wood (1995) in their scatter curve. This conclusion can only be avoided if the actual *flux* at eclipse minimum does not change much, leading to only small additive corrections. But then, the strongly varying eclipse depths seen at least in the present data suggests that Welsh & Wood (1995) would have measured the long-term variations instead of the flickering. Therefore, without knowledge of further details of their work the results of Welsh & Wood (1995) must be regarded with suspicion.

This shows how important – and dangerous – long term variations in the light curves are when applying the ‘ensemble’ method. Bennie et al. (1996) devised a way to overcome this problem and applied it to RW Tri. Unfortunately they published only a very concise and qualitative description of their method. Here, I will try to reconstruct it.

Due to the briefness of the presentation of Bennie et al. (1996) details of the reconstruction may differ from the original method. But this should not affect the basic idea. However, I will introduce one major difference: Bennie et al. (1996) (just as Horne & Stiening 1985 and Welsh & Wood 1995) expressed their light curves in fluxes, implying that they had calibrated them. The archival light curves for the present study (see Sect. 3) – all of them obtained with photon counting devices – are only available in count rates. They were observed at very different epochs with a variety of instruments. Thus, an otherwise desirable transformation into fluxes is unfortunately not possible. At least for objects (and instruments) furnishing a weak signal, Poisson noise is not negligible in the present context. Whereas it is not obvious how to handle this effect easily once the light curves have been transformed into fluxes, the above mentioned disadvantage is – however only slightly – made up for by the easy application of a Poisson noise correction if the light curves are given in count rates. For these reasons the formulation presented here is

expressed in terms of count rates and includes a correction for Poisson noise.

In the spirit of the ‘ensemble’ method the scatter as a function of orbital phase  $\phi$  can be expressed as:

$$\sigma(\phi) = \sqrt{\frac{1}{N(\phi) - 1}} \times \sqrt{\sum_{i=1}^{N(\phi)} \frac{1}{C_{i,\text{ref}}^2} \left\{ [\bar{C}_i(\phi) - C_i(\phi)]^2 - \frac{1}{\sqrt{n}} C_i(\phi) \right\}}. \quad (1)$$

Let us regard the individual terms of this equation. The index  $i$  stands for an individual light curve.  $C_{i,\text{ref}}$  is a “reference count rate”. It can be taken as the mean count rate in parts of the light curve  $i$  which are not disturbed by features such as an eclipse or orbital hump. In order to account for long term variations Bennie et al. (1996) assumed that *all variations not due to flickering scale linearly with the reference count rate*, i.e. that a relation exists such that  $\bar{C}_i(\phi) = a(\phi) + b(\phi) C_{i,\text{ref}}$ . Here  $\bar{C}_i(\phi)$  is the count rate which one would observe in the absence of flickering. Note that this is the basic assumption of the method! It is important to realize that the slope  $b$  of this relation is permitted to be a function of phase. Thus, each part of the light curve may scale in a different (but linear) way with the reference count rate.

The difference between the observed count rate  $C_i(\phi)$  and the count rate  $\bar{C}_i(\phi)$  predicted in the absence of flickering is then interpreted as being due to flickering. The square of this difference [i.e. of the expression enclosed in square brackets in Eq. (1)] is the contribution of light curve  $i$  to the variance around the mean light curve at phase  $\phi$ . It is biased by Poisson noise.

The variance  $\sigma_{i,\text{P}}^2(\phi)$  due to the latter effect is equal to the mean count rate at phase  $\phi$ . If the variations in the light curve in a small interval around  $\phi$  are dominated by Poisson noise  $\sigma_{i,\text{P}}^2(\phi)$  can be taken as the mean count rate within this interval. If it is dominated by flickering (i.e. by real variations of the system brightness),  $C_i(\phi)$  is the best estimate for  $\sigma_{i,\text{P}}^2(\phi)$ . In praxis, this does not make a significant difference, and I assume  $\sigma_{i,\text{P}}^2(\phi) = C_i(\phi)$ . However, this holds only true if the light curve has not been binned in phase. Otherwise,  $\sigma_{i,\text{P}}^2(\phi)$  is decreased by  $\sqrt{n}$  where  $n$  is the number of original data points (if the light curve is expressed in counts per integration time) or time units (if it is expressed in counts per time unit) in a phase bin. Thus, the second term in the curved brackets in Eq. (1) constitutes the correction for Poisson noise.

The total variance at phase  $\phi$  is then the sum of the individual terms divided by  $N(\phi) - 1$ , where  $N(\phi)$  is the number of light curves available at phase  $\phi$ . However, it would be misleading to take the straight mean because this would give exaggerated weight to those light curves which were observed at high count rates (e.g. with a larger telescope) because then the absolute numbers of  $\bar{C}_i(\phi)$  and  $C_i(\phi)$  would be large. An equal weight can be assigned to each light curve by dividing its contribution to the total variance by the square of the reference count rate.

The square root of the total variance is finally the scatter at the phase  $\phi$  which is now independent of the actual order of

magnitude of the count rates. Somewhat loosely spoken it can be regarded as the mean amplitude of the flickering in terms of the reference count rate. Its absolute value therefore depends on the strength of the flickering relative to the other light sources in the system.

## 2.2. The ‘single’ method

The ‘single’ method is described in detail by Bruch (1996) who applied it successfully to the dwarf nova Z Cha. The scatter as a function of orbital phase  $\phi$  is defined in this case as:

$$\sigma_n(\phi) = \frac{1}{N(\phi)} \sum_{i=1}^{N(\phi)} \frac{1}{\bar{\sigma}_i} \quad (2)$$

$$\times \sqrt{\frac{\sum_{j=1}^n [\tilde{C}_{i,j}(\phi) - C_{i,j}(\phi)]^2}{n-1} - \frac{\sum_{j=1}^n C_{i,j}}{n}}.$$

In contrast to the ‘ensemble’ method no mean light curve is calculated here. Instead, the scatter of the data points around a smoothed version (in the sense that variations considered to be due to flickering are removed but others such as eclipses and variations on longer time scales are preserved) of each individual light curve is taken to define the scatter curve.

Let  $C_i(\phi)$  be the original count rate of light curve  $i$  at phase  $\phi$  and  $\tilde{C}_i(\phi)$  the count rate of the smoothed light curve. Let there be  $n$  data points in a small interval  $\Delta\phi$  around phase  $\phi$ . The first term under the square root in Eq. (2) is then the variance of the data points of light curve  $i$  around the smoothed light curve in the interval  $\Delta\phi$ .

It is biased by Poisson noise, the contribution of which to the total variance is just the mean of the count rates within  $\Delta\phi$  (in contrast to the ‘ensemble’ method I assume here that the light curves are not binned; a corresponding correction would be trivial). Thus, the second term under the square root in Eq. (2) constitutes a correction for Poisson noise, and the square root itself as a function of  $\phi$  is the scatter curve of light curve  $i$ .

Before taking the mean of the individual scatter curves it is necessary to normalize them in order not to lend higher weight to light curves which happen to have been observed at higher count rates for instrumental reasons. As normalization factor the average  $\bar{\sigma}_i$  of the scatter of light curve  $i$  over all phases is taken. Finally, the normalized [thus the index  $n$  in Eq. (2)] mean scatter curve is the sum over all individual normalized curves, divided by the number  $N(\phi)$  of light curves contributing at phase  $\phi$ .

The critical point of the method is the construction of the smoothed light curve. It is important that the smoothing is homogeneous, i.e. to ensure that no part of the light curve (in particular the eclipse) is smoothed better or worse than the other parts because this would bias the scatter as a function of phase. A homogeneous smoothing can be achieved by binning the original light curve in suitable (fixed) phase bins and then performing a spline interpolation (better suited than a spline fit because it has fewer degrees of freedom and is thus less subject to arbitrariness) between the points of the binned light curve.

The method has two free parameters: (1) The interval  $\Delta\phi$  used to calculate the variance between the original and the smoothed light curve defines the resolution of the scatter curve. Of course, a high phase resolution is always desirable but in praxis it is limited by the phase resolution of the original light curves and the acceptable statistical noise in the final scatter curve. (2) The phase interval over which the original light curves are binned before the smoothed light curve is calculated. Obviously the smoothed curve will follow variations on scales longer than the bin width which consequently will not contribute to the scatter. The choice of the appropriate bin width requires a balance between the maximum time scale of the flickering which is to remain detectable and the necessity for the spline to follow well the eclipse profile. The latter requirement sets an upper limit for the permissible bin width. The lack of sensitivity for flickering on time scales longer than the bin width is the main disadvantage of the ‘single’ method<sup>1</sup>. Its main advantage, on the other hand, is its robustness against long term variations of the regarded system. Since the scatter of each individual light curve is calculated (before taking the mean) all long term variations are eliminated when the difference curve  $\tilde{C}_i(\phi) - C_i(\phi)$  is constructed. This is in contrast to the ‘ensemble’ method where variations on long time scales (or even non-repetitive variations on orbital time scales) represent a major difficulty.

## 2.3. Application to artificial light curves

In order to test the validity of the concepts described in Sects. 2.1 and 2.2 they will first be applied here to artificial light curves before real data are subjected to them. 100 light curves with artificial flickering based on a shot noise model were generated. Their mean count rates varied randomly between 1000 and 2000 (i.e. in a realistic range but not too large for Poisson noise to become negligible). Each light curve contains an eclipse in the phase interval  $-0.05 \leq \phi \leq 0.05$  with a constant residual count rate of 10% of the mean out-of-eclipse count rate. During eclipse ingress ( $-0.15 \leq \phi \leq -0.05$ ) the mean count rate drops linearly and the weight of the flickering drops from 1 at  $\phi = -0.15$  to 0 at  $\phi = -0.05$  during this interval. Eclipse egress is simulated in an analogous manner at  $0.05 \leq \phi \leq 0.15$ . An orbital hump was introduced as the positive half of a sine curve in the interval  $-0.50 \leq \phi \leq -0.05$ . For each of the hundred light curves its amplitude is a random number between 0 and the mean count rate in the interval  $0.15 \leq \phi \leq 0.50$ . Finally, Poisson noise was simulated by adding to each data point a random number drawn from a Gaussian distribution (good enough an approximation for a Poissonian distribution at the assumed count rates) with a mean of 0 and a standard deviation equal to the value of the data point itself. An example of such an artificial light curve is shown in Fig. 1a.

<sup>1</sup> This is also the reason to choose a normalization for the scatter curve which cannot be interpreted in terms of the amplitude of the flickering relative to the background light as in my formulation of the ‘ensemble’ method: Any such interpretation would be misleading because the (generally) stronger flickering on longer time scales might not be seen with the ‘single’ method.

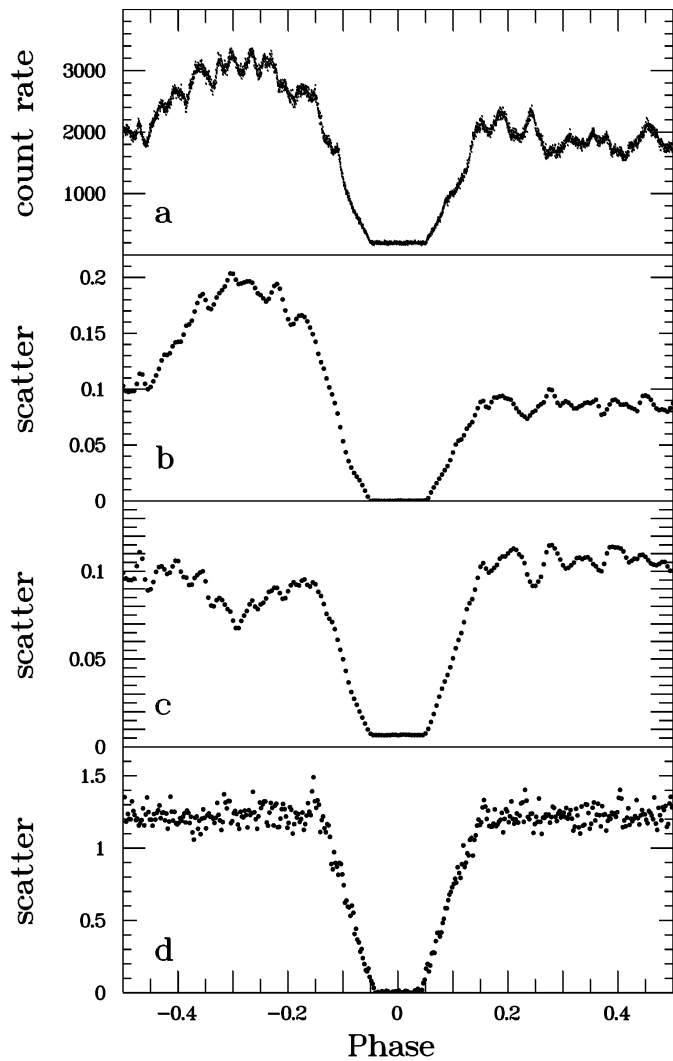


**Fig. 1.** **a** An example of an artificial flickering light curve with eclipse. **b** Scatter curve of an ensemble of 100 artificial light curves calculated with the ‘ensemble’ method. The reference flux was defined as the mean count rate in the range  $0.15 \leq \phi \leq 0.5$ . **c** Same as above with the reference flux defined in the range  $-0.35 \leq \phi \leq -0.2$ . **d** Scatter curve of the same ensemble of artificial light curves calculated with the ‘single’ method.

Before applying the ‘ensemble’ method to these data they were binned in intervals of  $\Delta\phi = 0.005$ . The reference flux was taken to be the mean count rate in the interval  $0.15 \leq \phi \leq 0.5$  (i.e. disregarding eclipse and hot spot). The resulting scatter curve is shown in Fig. 1b. As expected, during eclipse the scatter is reduced to 0. During egress it rises constantly; the giggles are due to the progressively visible flickering light source. After egress, the scatter remains on a more or less constant level. However, what happened at phases before the eclipse? There is a hump reflecting the orbital hump although the simulated flickering strength at these phases is the same as after the eclipse. The answer is simple: During the construction of the light curves the hump amplitude (relative to the mean count rate at phase  $0.15 \leq \phi \leq 0.5$ ) was varied in a manner completely indepen-

dent of the mean count rate. Thus, the basic assumption of the ‘ensemble’ method is violated, namely that all variations not due to flickering scale linearly with the reference flux. If, on the other hand, the variations of the hump amplitude are considered as flickering, the hump in the scatter curve is perfectly as expected: It then reflects the enhanced scatter due to this additional flickering component.

In order to study the effect of an unsuitable choice of the reference flux the calculations were repeated using as reference flux the mean count rate in the interval  $-0.35 \leq \phi \leq -0.2$ , i.e. right on top of the (variable) hump. The results, shown in Fig. 1c, could have been foreseen: The scatter assumes a minimum at the phases where  $F_{\text{ref}}$  was defined while it is augmented at other (out-of-eclipse) phases. The eclipse bottom is somewhat elevated, but not enough to significantly alter the properties of the scatter eclipse.

Finally, Fig. 1d shows the scatter curve of the same sample of artificial light curves, calculated with the ‘single’ method. Obviously, the scatter conforms perfectly well with the expectations with the exception of a slightly too small eclipse width. This is an artifact explained by the discontinuous transition between the ingress/egress slopes and the constant eclipse bottom which cannot be followed by the smoothed light curve. The orbital hump is not seen in the scatter curve because it is connected with variations well above the time scale for which the ‘single’ method is sensible. Whether this is desirable or not depends on the point of view: Should orbital variations of the hump amplitude be regarded as flickering or not?

#### 2.4. Application to HT Cas

In the previous section it was shown that in the case of artificial light curves with well defined properties both methods yield the expected results within their respective limitations. Now, the ‘ensemble’ method will be applied to real light curves of the dwarf nova HT Cas (the application of the ‘single’ method to the same data will follow in Sect. 4.1).

Since HT Cas does not show a strong orbital hump, and since the effect of an unsuitable choice of  $C_{\text{ref}}$  on the scatter eclipse is limited, the entire light curve with the exception of the eclipses ( $-0.05 \leq \phi \leq 0.05$ ) was used to define  $C_{\text{ref}}$ . The resulting curve is shown in Fig. 2c. It has no resemblance with the corresponding curve calculated with the ‘single’ method (Sect. 4.1, Fig. 3). In particular, no trace of a scatter eclipse is visible. Quite on the contrary! This can be understood regarding the three exemplary light curves of HT Cas (binned in phase for clarity but not altered concerning their count rates) in Fig. 2b. The count rates out of eclipse are not proportional to those at the minima. Thus, the basic assumption of the ‘ensemble’ method is violated. This is underlined by the relation between the reference count rate and the count rate at eclipse minimum shown in Fig. 2a (here, the data points representing the light curves shown in the middle frame are ringed). It is obvious that both quantities are not proportional to each other but only loosely correlated.

In principle the violation of the basic assumption could be due to the fact that the light curves are expressed in count rates

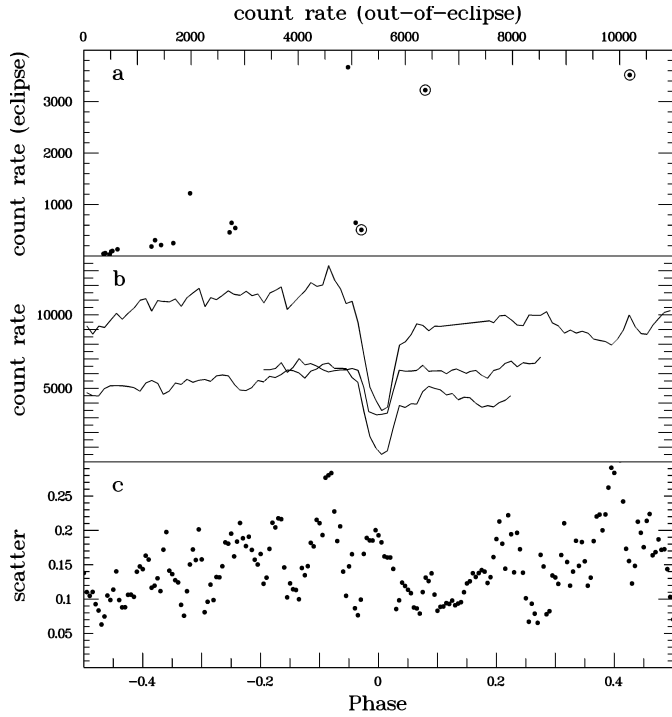


**Fig. 2.** **a** Count rates of the light curves at HT Cas at eclipse bottom as a function of the out-of-eclipse count rate. The ringed data points correspond to the light curves shown in the next frame. **b** Three light curves of HT Cas, binned in phase for clarity but unaltered concerning the count rates. **c** Scatter curve of HT Cas calculated using the ‘ensemble’ method.

rather than in fluxes. As was detailed in Sect. 2.1 the method assumes that long term variations at a given phase scale linearly with the reference count rate. In the present context variations of the count rates may be due to real long term variations as well as to different instrumental setups. The latter would cause the same relative variation at all phases while for the former the relative variations can be phase dependent. Thus, mixing real long term variations and such due to instrumental effects causes a superposition of two different equations of the kind  $\bar{C}_i(\phi) = a(\phi) + b(\phi) C_{i,\text{ref}}$  (see Sect. 2.1), resulting in an apparently enhanced scatter.

Although this effect may contribute to the failure of the ‘ensemble’ method in the present case it is certainly not the principle reason. The strongly variable eclipse depth in HT Cas with respect to the out-of-eclipse light level is independent of the absolute value of the count rates and would clearly lead to a strong scatter during eclipse even if the light curves were expressed in fluxes.

Application of the ‘ensemble’ method to light curves of UX UMa (Sects. 3 and 4.4) led to a similar failure.

### 2.5. Conclusions

Although the ‘ensemble’ method is quite appealing at first glance, and although its first application by Horne & Stiening (1985) met success, its application is

limited to “well behaved CVs”. This term, however, is almost a contradiction in itself. As was pointed out by Welsh et al. (1996) the sensitivity of the ‘ensemble’ method to violations of stationarity is a major disadvantage. This does not mean that it cannot yield useful results under carefully chosen and controlled circumstances which, however, for the large majority of CVs will be difficult to realize. In view of the additional difficulties arising from the fact that the light curves available for the present study are all uncalibrated the application of the ‘ensemble’ method to these data is definitely not suitable. Therefore, the ‘single’ method is preferred here.

Doubtlessly, the ‘single’ method also has its drawbacks: It yields rather noisy scatter curves unless the number of light curves is exceedingly high, and it is insensitive to flickering on time scales longer than those of the remaining variations in the smoothed light curves. However, as has been shown by Bruch (1996), Bruch et al. (2000) and will be shown in Sect. 4 of the present paper, it is capable to produce useful scatter curves of the flickering even for the most unstationary CVs.

### 3. The observational material

For the present study only archival light curves of the four systems HT Cas, V2051 Oph, IP Peg and UX UMa observed at the SAAO, South Africa, at the MacDonald Observatory, USA, and at the Wise Observatory, Israel, were used. Most of the data of HT Cas and V2051 Oph were already studied with respect to other properties than the flickering. With the exception of two so far unpublished light curves the data of HT Cas were published by Patterson (1981) and Zhang et al. (1986). Of V2051 Oph, 6 light curves are unpublished; the others can be found in Warner & Cropper (1983) and Warner & O’Donoghue (1987). The quoted references also contain details about the observations. In contrast, none of the light curves of IP Peg and UX UMa used here was published to my knowledge.

The large majority of the data refers to white light, but a few light curves were observed with the four channel Stiening photometer (Horne & Stiening 1985). In these cases only the *B* band was employed. The brightness of the stars is given as counts per integration time, corrected for extinction and sky background. The latter features imply that only an approximate correction of the scatter curves for Poisson noise is possible. However, this does not affect the results seriously (see Bruch 1996 for a discussion of this point). For the three dwarf novae in the present sample (HT Cas, V2051 Oph and IP Peg) only light curves obtained during quiescence are used.

The amount of available data differs very much for the four stars investigated here. Whereas data of 66 orbital cycles were used in the case of V2051 Oph, the corresponding numbers for HT Cas, UX UMa and IP Peg are 22, 9 and 3. Since the dependence of the scatter in the light curves is to be studied here as a function of orbital phase all light curves were phase folded (after splitting those light curves containing more than one cycle into separate curves). Table 1 contains an overview: The individual columns list the cycle number, the heliocentric Julian Date of the corresponding eclipse, the civil date, and the

**Table 1.** Eclipse numbers, Julian dates, civil dates and time resolution for the light curves used in this study

E	HJD 2440000+	civil date	$\Delta t$ (sec)	E	HJD 2440000+	civil date	$\Delta t$ (sec)	E	HJD 2440000+	civil date	$\Delta t$ (sec)
HT Cas:				V2051 Oph (cont.):				V2051 Oph (cont.):			
0	3727.93721	1978/ 8/ 7	3	4873	5091.53210	1982/ 5/ 2	5	17446	5876.43759	1984/ 6/24	3
448	3760.93116	1978/ 9/ 9	3	5145	5108.51248	1982/ 5/19	5	17460	5877.31158	1984/ 6/25	3
461	3761.88857	1978/ 9/10	3	5207	5112.38301	1982/ 5/22	5	17461	5877.37400	1984/ 6/25	3
462	3761.96222	1978/ 9/10	3	5223	5113.38185	1982/ 5/23	5	17462	5877.43643	1984/ 6/25	3
733	3781.92061	1978/ 9/30	3	5289	5117.50209	1982/ 5/28	10	17463	5877.49886	1984/ 6/25	3
1599	3845.69909	1978/12/ 3	5	5336	5120.43620	1982/ 5/30	10	17475	5878.24799	1984/ 6/26	5
1600	3845.77274	1978/12/ 3	5	5351	5121.37262	1982/ 5/31	10	17476	5878.31042	1984/ 6/26	5
1897	3867.64896	1978/12/25	8	5352	5121.43505	1982/ 5/31	1	17477	5878.37285	1984/ 6/26	5
1898	3867.71963	1978/12/25	8	15591	5760.63391	1984/ 3/ 1	5	17478	5878.43528	1984/ 6/26	5
1993	3874.71609	1979/ 1/ 1	3	16632	5825.62131	1984/ 5/ 5	5	17492	5879.30927	1984/ 6/27	5
5105	4103.90619	1979/ 8/18	8	16676	5828.36813	1984/ 5/ 7	5	17572	5884.30350	1984/ 7/ 2	5
6853	4232.64150	1979/12/25	4	16677	5828.43056	1984/ 5/ 7	5	17573	5884.36592	1984/ 7/ 2	5
6854	4232.71515	1979/12/25	4	16678	5828.49299	1984/ 5/ 7	5	18293	5929.31398	1984/ 8/16	5
20773	5257.81058	1982/10/15	2	16679	5828.55542	1984/ 5/ 8	5	18294	5929.37641	1984/ 8/16	5
20786	5258.76799	1982/10/16	1	16680	5828.61785	1984/ 5/ 8	5	24044	6288.33661	1985/ 8/10	1
20787	5258.84164	1982/10/16	1	16694	5829.49184	1984/ 5/ 8	10	24045	6288.39903	1985/ 8/10	1
20813	5260.75647	1982/10/18	1	16695	5829.55426	1984/ 5/ 9	10	24156	6295.32853	1985/ 8/17	5
20828	5261.86118	1982/10/19	1	16696	5829.61669	1984/ 5/ 9	10				
21573	5316.72834	1982/12/13	1	17031	5850.53002	1984/ 5/30	5				
21598	5318.56952	1982/12/15	2	17032	5850.59245	1984/ 5/30	5	IP Peg:			
21599	5318.64317	1982/12/15	2	17045	5851.40401	1984/ 5/30	5	?	? 1990/10/26	2	
21600	5318.71682	1982/12/15	2	17046	5851.46644	1984/ 5/30	5	?	? 1990/10/26	2	
				17047	5851.52887	1984/ 5/31	5	21101	8953.73058	1992/11/27	1
				17061	5852.40286	1984/ 5/31	5				
V2051 Oph:				17062	5852.46529	1984/ 5/31	5				
								UX UMa:			
-23044	3348.73354	1977/ 7/24	3	17063	5852.52772	1984/ 6/ 1	5				
-17933	3667.80233	1978/ 6/ 8	3	17064	5852.59014	1984/ 6/ 1	5	-6897	2548.43692	1975/ 5/15	5
-16910	3731.66603	1978/ 8/11	4	17078	5853.46413	1984/ 6/ 1	5	-6892	2549.42027	1975/ 5/16	5
-11807	4050.23540	1979/ 6/26	4	17079	5853.52656	1984/ 6/ 2	5	-6887	2550.40363	1975/ 5/17	4
0	4787.32114	1981/ 7/ 1	5	17080	5853.58899	1984/ 6/ 2	5	-6882	2551.38698	1975/ 5/18	5
								-3016	3311.71815	1977/ 6/17	5
1	4787.38357	1981/ 7/ 1	5	17396	5873.31619	1984/ 6/21	3				
17	4788.38241	1981/ 7/ 2	5	17429	5875.37631	1984/ 6/23	3	477	3998.69092	1979/ 5/ 5	5
18	4788.44484	1981/ 7/ 2	5	17430	5875.43874	1984/ 6/23	3	482	3999.67428	1979/ 5/ 6	5
64	4791.31652	1981/ 7/ 5	5	17431	5875.50117	1984/ 6/24	3	487	4000.65763	1979/ 5/ 7	5
4265	5053.57596	1982/ 3/25	5	17443	5876.25030	1984/ 6/24	3	24787	8779.76969	1992/ 6/ 6	1
4329	5057.57135	1982/ 3/29	5	17444	5876.31273	1984/ 6/24	3				
4872	5091.46967	1982/ 5/ 1	5	17445	5876.37516	1984/ 6/24	3				

time resolution of the light curves in seconds. The phase coverage of the individual cycles is not always complete. Whereas for HT Cas and V2051 Oph in most cycles the complete phase range  $-0.5 \leq \phi \leq 0.5$  around the eclipses is covered, in the longer period system UX UMa in general only a restricted phase range centered on the eclipse was observed.

The cycle numbers and the corresponding eclipse numbers quoted in Table 1 are based on the ephemeris of Horne et al. (1991) in the case of HT Cas, Echevarría & Alvarez (1993) for V2051 Oph and Baptista et al. (1995) for UX UMa. The orbital period of IP Peg is not stable as was first pointed out by

Wood et al. (1989b). Wolf et al. (1993) later found the period variations to be cyclic. Here, the ephemeris of Wolf et al. (1993) are adopted. However, in two cases none of the published ephemeris predicts the epochs of the minima observed in the present light curves even approximately. There may be a timing error. Therefore, no cycle numbers and eclipse epochs are given for these cases in Table 1.

Not in all cases the eclipse epochs predicted from the ephemeris matched well the observed eclipses. Instead of trying to trace the reasons for the inconsistencies (difficult in view of the limited information available about the observational details

of the archival data) a pragmatic approach was adopted: In such cases, the epoch of the eclipse centre was visually measured in the light curve (sufficient to ensure an accuracy which is higher than the phase resolution of the final scatter curves), and the phase-folding was done using that epoch as zero-point.

#### 4. The scatter curves

The mean scatter curves for HT Cas, V2051 Oph, IP Peg and UX UMa were calculated using the ‘single’ method. A bin width of 0.01 in phase was used for all stars when calculating the smoothed light curve (see Sect. 2.2). Therefore, only flickering occurring on time scales below roughly 1<sup>m</sup> for HT Cas and V2051 Oph, 2<sup>m</sup> for IP Peg and 3<sup>m</sup> for UX UMa is seen.

##### 4.1. HT Cas

HT Cas belongs to the SU UMa subclass of CVs. In the prototypical eclipsing members of this group the light curves exhibit a strong orbital hump and the eclipse profile permits to separate the eclipse of the white dwarf and of the hot spot (OY Car: Wood et al. 1989a; Z Cha: Wood et al. 1986). In this respect HT Cas is rather unstable: An orbital hump is sometimes present; at other epochs no trace of it is visible. It is never as prominent as in OY Car and Z Cha. Similarly, the eclipse profiles may or may not show the typical structure caused by a white dwarf eclipse, followed slightly later by a hot spot eclipse (see e.g. Fig. 8 of Patterson 1981). A representative light curve and the mean of all curves studied here (normalized to a common mean count rate) are shown in Figs. 3a and 3b. There is no significant orbital hump in the mean curve, and the eclipse profile contains at most a remnant of a two-step eclipse (white dwarf and hot spot). Thus, on the average the hot spot has no significant influence on the light curve shape in the present data.

When applying the ‘single’ method to the HT Cas light curves it was found that due to the very sudden start and end of the white dwarf eclipse ingress and egress and to the short duration of these phases the spline interpolation to the binned light curve (performed as outlined by Bruch 1996) could not follow well the eclipse ingress and egress, causing large residua in the difference curve at these phases. These translated into artificial peaks in the scatter curve. To alleviate this problem additional fiducial points for the spline interpolation were defined interactively at the beginning and end of the steep parts of eclipse ingress and egress. While this significantly reduced the height of the sharp peaks in the scatter curve, it could not remove them completely.

The resulting scatter curve, calculating the scatter in phase intervals of width 0.005 and adopting a step-width of 0.0025 (meaning that neighbouring points in the scatter curve are not independent of each other) is shown in Fig. 3c. Each point in the final scatter curve is the mean value of several individual curves. An error of  $\sigma/\sqrt{m}$  (“mean error of the mean”) is assigned to each point, where  $m$  is the number of individual points contributing to the mean, and  $\sigma$  is the standard deviation. The representative error bar shown in the upper left corner of Fig. 3c

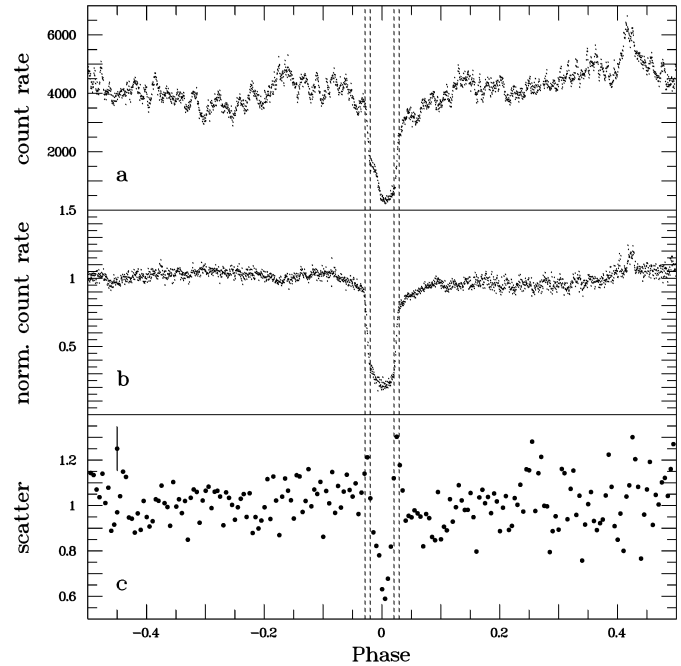


**Fig. 3.** **a** Representative light curve of HT Cas. **b** Normalized mean orbital light curve of HT Cas. **c** Mean scatter curve of HT Cas. The dashed vertical lines indicate the contact phases of the white dwarf eclipse as measured by Horne et al. (1991). A representative error bar is shown in the upper left corner.

is the average value (= 0.097) of the errors of all data points. The dashed vertical lines are the eclipse contact phases of the white dwarf as measured by Horne et al. (1991). It is seen that – disregarding the artificial peaks occurring during eclipse ingress and egress – the minimum of the scatter curve coincides with the eclipse of the white dwarf. Thus, the flickering light source in HT Cas is well centered on the central body.

Although it may not be very significant in view of the noise in the scatter curve, the scatter eclipse appears to be V-shaped rather than flat-bottomed. If this is true it would mean that the flickering light source is a bit larger in extension than the white dwarf itself. However, it cannot be much larger because otherwise the ingress of the scatter eclipse should start earlier (and end later) than the white dwarf eclipse as the secondary star covers more and more of the region where flickering occurs. This is not seen.

There is no significant enhancement of the scatter during the phase interval in which the canonical hot spot is visible in many CVs. Thus the region of impact of the transferred matter onto the accretion disk appears not to host a flickering light source in HT Cas. The lack of any systematic trend of the scatter which phase (except for the eclipse) is formally confirmed by a Gauss fit to a histogram of the (out-of-eclipse) data points which yields a standard deviation of 0.101, almost identical to the average mean error of the data points of 0.097. This constancy of the scatter (disregarding the eclipse) is different from what is found for e.g. Z Cha (Bruch 1996), V893 Sco (Bruch et al. 2000) and IP Peg (see Sect. 4.3).

The present quantitative results are in agreement with qualitative conclusions of Patterson (1981), namely that the flickering in HT Cas originates from regions very close to the white dwarf.

#### 4.2. V2051 Oph

Even disregarding the strong flickering activity, V2051 Oph has the most unstable light curve of all stars considered here. During most cycles, a hump is clearly present. However, its amplitude is quite variable, and in some cycles it all but vanishes. Moreover, its phase is not stable: While in most cycles its maximum occurs before the eclipse (as is expected for an orbital hump caused by the hot spot) sometimes it coincides with the eclipse or wanders to even later phases. Moreover, with a considerable frequency an intermediate hump appears roughly half a cycle before (or after) the principle hump.

The latter, however, disappears in the mean light curve which is shown together with a representative individual curve in of Figs. 4b and 4a, respectively. The mean hump is located at its canonical phase and has a moderate amplitude (as compared to e.g. Z Cha, Wood et al. 1986, or IP Peg, Sect. 4.3). Note also that in contrast to other eclipsing systems with prominent humps the end of the hump occurs even before the onset of the eclipse. However, this is only true for the mean curve and may be quite different in individual cycles. The mean eclipse profile differs from that of HT Cas (Sect. 4.1). It does not show the sudden eclipse ingress and egress of the white dwarf (although this may still be visible in individual light curves; Warner & Cropper 1983) but is more gradual. This, together with the round eclipse bottom, points towards a higher contribution of the accretion disk which is never totally eclipsed in this system. During an exceptionally low state of V2051 Oph Baptista et al. (1998) were able to measure the contact points of white dwarf eclipse ingress and egress. The corresponding phases are indicated by the dashed vertical lines in Fig. 4.

The scatter curves for the individual light curves were calculated as in the case of HT Cas. The resulting mean curve is shown in Fig. 4c. The average error of the data points of 0.064 is shown in the lower right corner. The eclipse is similar to that observed in HT Cas but – due to the much larger number of individual light curves and the absence of the problems with the steep eclipse ingresses and egresses – much better defined. In particular, the scatter eclipse is coincident with the white dwarf eclipse and definitely narrower than the disk eclipse. Thus, also in this system the flickering light source is located very close to the white dwarf while the outer parts of the accretion disk do not take part in the flickering to a perceptible degree.

In contrast to HT Cas, however, the scatter curve shows evidence that flickering occurs also to a certain degree at the location of the impact of the transferred matter onto the accretion disk: the scatter is clearly elevated at the phases when the orbital hump is visible. This is formally confirmed by the standard deviation of 0.080 of a Gauss fit to the histogram of the out-of-eclipse data points which is larger than their average mean error of 0.064. This hot spot flickering can also explain the appar-

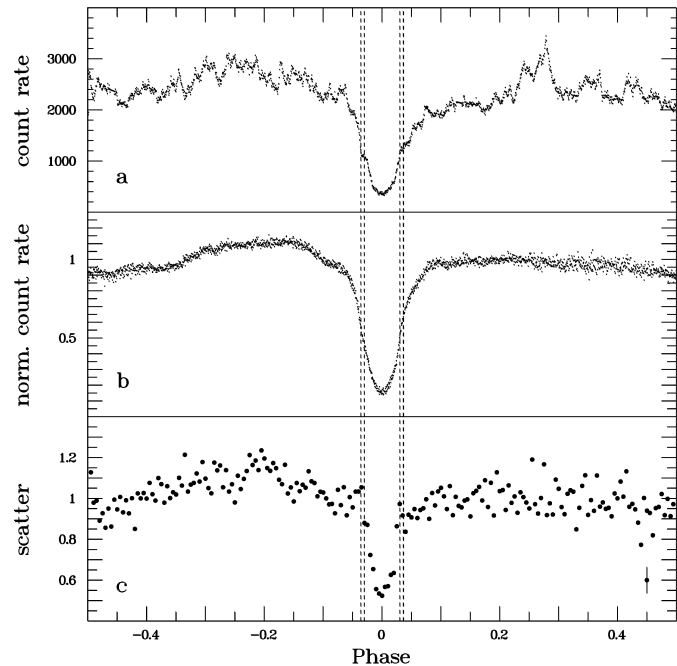


**Fig. 4.** **a** Representative light curve of V2051 Oph. **b** Normalized mean orbital light curve of V2051 Oph. **c** Mean scatter curve of V2051 Oph. The dashed vertical lines indicate the contact phases of the white dwarf eclipse as measured by Baptista et al. (1998). A representative error bar is shown in the lower right corner.

ent slight asymmetry of the scatter eclipse: it remains visible for a short time even after the white dwarf is already eclipsed, causing a slightly more gradual eclipse ingress, but is invisible when the central star emerges from the eclipse, explaining the steeper scatter eclipse egress. This behaviour of the flickering in V2051 Oph is identical to that of Z Cha during quiescence as measured by Bruch (1996).

The present results are in excellent agreement with those of Warner & Cropper (1983). They concluded “that in V2051 Oph the flickering is probably in general generated in the inner disk region with only a minor contribution from the hot spot”.

#### 4.3. IP Peg

The light curves of IP Peg differ strongly from those of HT Cas and V2051 Oph. As an example the *B* light curve (Stiening system) of 1992, November 27, is shown in Fig. 5a. It is dominated by an exceptionally strong hump which reaches a peak flux approximately three times as high as the flux at phase  $\approx -0.4$  where the hump is invisible. The eclipse is characteristically structured: A steep part of the ingress caused by the white dwarf ingress is followed by a more gradual part due to the hot spot ingress. Unlike in the classical SU UMa systems OY Car and Z Cha, however, white dwarf and hot spot ingress cannot be separated. The white dwarf egress is in most cycles discernible as a discrete step in the light curve. Somewhat later a second step marks the egress of the hot spot.

In view of the variations of the location of the hot spot in the system the corresponding contact phases are not very sta-

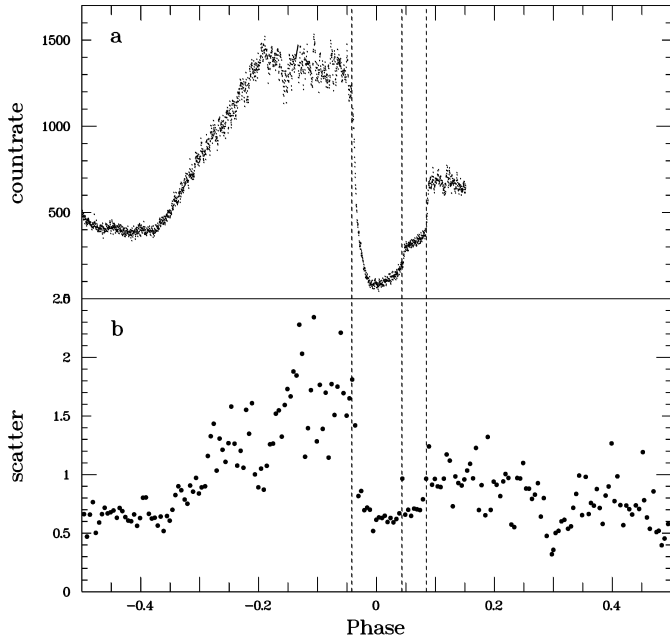


**Fig. 5.** **a** *B* light curve of IP Peg of 1992, November 27. **b** Mean scatter curve of IP Peg. The lateral dashed vertical lines indicate the first and last contact points of the hot spot eclipse, while the central lines marks white dwarf eclipse egress phase as measured by Wood et al. (1989b).

ble as was shown by Wood et al. (1989b). The lateral dashed lines in Fig. 5 represent the mean first and last hot spot eclipse contacts as measured in the present light curves. The central line marks the mean white dwarf egress phase determined by Wood et al. (1989b).

The general character of the short term variations of IP Peg is different from that of other CVs. Significant variations above the noise level are only seen during the presence of the orbital hump, suggesting that the hot spot is the culprit. This is confirmed by the more formal scatter analysis.

The mean scatter curve of IP Peg (Fig. 5b) was measured in the same way as in the previous cases. Since it is based on only three light curves the noise is particularly large. For the same reason it is not sensible to derive formal errors in the way done for the other stars in this study. Nevertheless there is no doubt that it is significantly different from the corresponding curves for the other stars. The strong increase of the scatter at the phases when the orbital hump is visible indicates that the flickering in IP Peg is dominated by the hot spot. In contrast to Z Cha (Bruch 1996) and V2051 Oph (Sect. 4.2) where the scatter eclipse ends with the white dwarf eclipse even if the hot spot continues to be eclipsed, there is no significant increase of the scatter of IP Peg when the white dwarf eclipse ends. The scatter only increases when the hot spot emerges from the eclipse (the single high point just at white dwarf egress is an artifact due to the same effect which produces the spurious peaks in the HT Cas scatter curve; see Sect. 4.1).

Recognizing that the scatter at phases when the hot spot is invisible is as small as during eclipse centre indicates that in

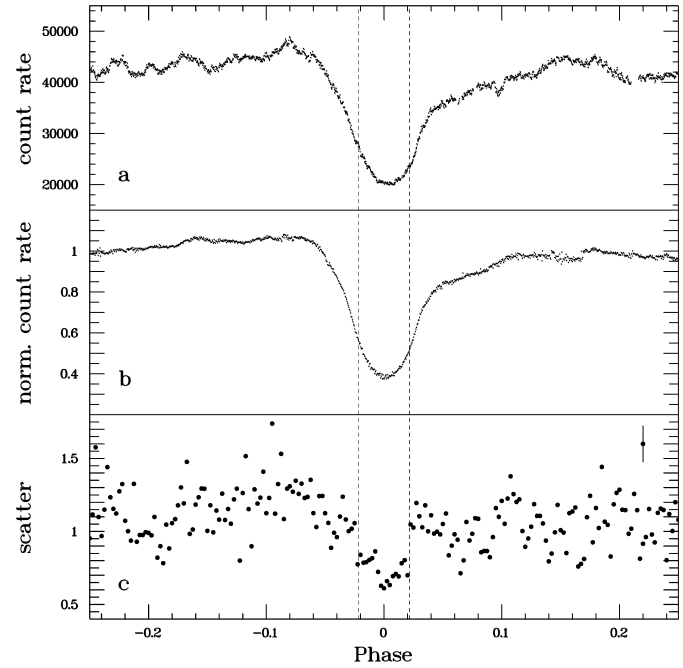


**Fig. 6.** **a** Representative light curve of UX UMa. **b** Mean light curve of UX UMa. **c** Mean scatter curve of UX UMa. The dashed vertical lines indicate the white dwarf eclipse ingress and egress phases as measured by Baptista et al. (1995). A representative error bar is shown in the upper right corner.

this particular system the accretion disk/white dwarf contributes practically nothing to the total flickering.

Since these conclusions are based on only three light curves, they may not be as firm as concerning the other stars of this study. However, it does not appear likely that the light curves used here which are very similar to each other are wholly atypical for IP Peg.

#### 4.4. UX UMa

Due to the longer orbital period the phase coverage of the presently available light curves of UX UMa is not as complete as for the other stars in this study. Therefore, the phase range for the present investigations is restricted to  $-0.25 \leq \phi \leq 0.25$ . A representative individual light curve and the mean of all normalized curves are shown in Figs. 6a and 6b, respectively (note that the discontinuity in the mean curve close to phase  $\phi = 0.17$  is an artifact caused by a light curve with a particularly low light level after eclipse which contributes to the mean only at phases  $\phi \leq 0.17$ ). The broadness of the eclipse and the rounded bottom suggests that the eclipsed body is extended (the accretion disk) and that it is never fully eclipsed. This agrees with the low orbital inclination of  $70^\circ 0 \pm 0^\circ 6$  determined by Baptista et al. (1995), which is just high enough to cause grazing eclipses of the white dwarf. Using UV light curves, Baptista et al. (1995) could also measure the white dwarf eclipse ingress and egress phases which are marked in Fig. 6 by dashed vertical lines. The eclipse contains an extended wing at egress, a feature introduced by the

retarded eclipse egress of the hot spot. The presence of the latter is also visible in eclipse maps of UX UMa (Baptista et al. 1995).

The mean scatter curve, calculated in the same way as in the previous cases, is shown in Fig. 6c. The average mean error of the data points (upper right corner of Fig. 6c) is 0.125. Although the scatter curve is rather noisy there is no doubt about the presence of an eclipse. Once again, its boundaries agree remarkably well with those of the white dwarf eclipse, indicating that in UX UMa (as in HT Cas and V2051 Oph) the flickering light source is located very close to the central body. Using the orbital inclination of  $70^\circ$ , a mass ratio of 1 (Baptista et al. 1995) and taking into account the distorted shape of the Roche-lobe filling secondary star it is found that the secondary star eclipses the accretion disk on the far side only out to  $\approx 4.4$  white dwarf radii. Therefore, the flickering light source – at least a significant part of it – must be located within this distance for a sharply confined flickering eclipse to occur. In view of the scatter of the curve and the unknown contribution of residual noise (Bruch 1996) no attempt is made here to quantify this statement. However, the extremely rapid eclipse egress permits an even considerably narrower distribution of the flickering around the white dwarf. The apparently more gradual eclipse ingress and the slightly enhanced scatter before the eclipse (the Gauss fit to the histogram of all out-of-eclipse points yields a standard deviation of 0.185, significantly larger than the average mean error of 0.125) may also in this case indicate a hot spot contribution to the total flickering.

## 5. Discussion and conclusions

The term “flickering” has never been well defined. In particular, it is not clear whether variations occurring on time scales of hours (or orbital time scales) and those on minute time scales should be regarded as different aspects of the same phenomenon. If this is the case one might expect that the time scales on which the individual events of the flickering develop are drawn from a common, albeit unknown distribution function. If, on the other hand, variations on largely different time scales are due to different physical mechanisms the respective durations will in general be drawn from different distribution functions.

While the statistical superposition of many events makes it impractical to determine the distribution functions directly, a look at the auto-correlation-functions (ACFs) of CV light curves might be helpful. Therefore the ACFs of several hundred light curves of dozens of CVs have been calculated. In the majority of them a common feature can be discerned more or less clearly. As examples, the upper three frames of Fig. 7 contain exemplary light curves with their respective ACFs of three different systems. All ACFs show a narrow central maximum<sup>2</sup> with a half width of several minutes at its base (the exact value can vary between  $\sim 3$  minutes and  $\sim 20$  minutes and appears to be char-

acteristic for each system). This maximum is superposed on a broader base which itself may be structured (but note that ACF structures on times scales not short compared to the duration of the light curve are easily dominated by the accidental presence of randomly distributed features occurring on such longer time scales).

The distinction between the narrow maximum and the broad base suggests that variations with different distributions functions for their respective time scales are superposed. In order to test if this conclusion is reasonable an artificial light curve was constructed which consists of a superposition of two ensembles of flares with different distribution functions concerning their amplitudes and time-scales. The light curve is shown together with its ACF in the lower frame of Fig. 7. The structure of the ACF is very similar to that of the ACFs of the real light curves. While this is not a rigorous proof that the variations in CV light curves are in fact governed by events drawn from different distribution functions, it lends credibility to this conjecture.

If this is true variations on different time scales must be expected to be due to different physical mechanisms. They should therefore not be labelled by the same term. I suggest to use the term “flickering” only for those variations which cause the above mentioned narrow maximum in the ACFs.

These ideas have some bearing on the interpretation of the results of Sect. 4: The lack of sensitivity for variations on time scales longer than the bin width of the smoothed light curves was mentioned in Sect. 2.2 as the main disadvantage of the ‘single’ method. However, even if the ‘single’ method does not see the bulk of the power of the flickering (which is emitted in flares occurring in general on time scales longer than the acceptable bin width) it is sensitive to variations drawn from the same distribution of time scales. Therefore, unless variations drawn from different parts of the distribution are not co-spatial, the part of the flickering sampled by the ‘single’ method is representative for the entire flickering in terms of its location.

It is striking that in all of the present cases as well as in Z Cha (Bruch 1996) (with the exception of the superoutburst state) and V893 Sco (Bruch et al. 2000) the phases of start and end of the scatter eclipse coincide to within the resolution of the scatter curves with eclipse ingress and egress of well defined light sources in the respective systems, be it the white dwarf or the hot spot. This is true also for V2051 Oph and UX UMa where the mean light curves do not show sharp ingress or egress features at these phases, lending confidence that the scatter eclipses are not caused by some hidden effect of the adopted method.

These results leave little doubt as to the place of origin of the flickering. It can arise in two regions: The innermost accretion disk including the boundary layer and the surface of the white dwarf itself (the phase resolution of the scatter curves does not permit to distinguish these regions), and the region of impact of the stream of matter transferred from the secondary star upon the accretion disk. The relative strength of what might be termed hot spot flickering and white dwarf flickering (Bruch 1996) can vary from one object to the other. Whereas in HT Cas the hot spot does not contribute perceptibly to the flickering, in V2051 Oph,

<sup>2</sup> This maximum is not to be confused with the unresolved central spike best seen in the ACF of the GK Per light curve. The latter feature is an artifact due to statistical noise which only correlates at zero time lag.

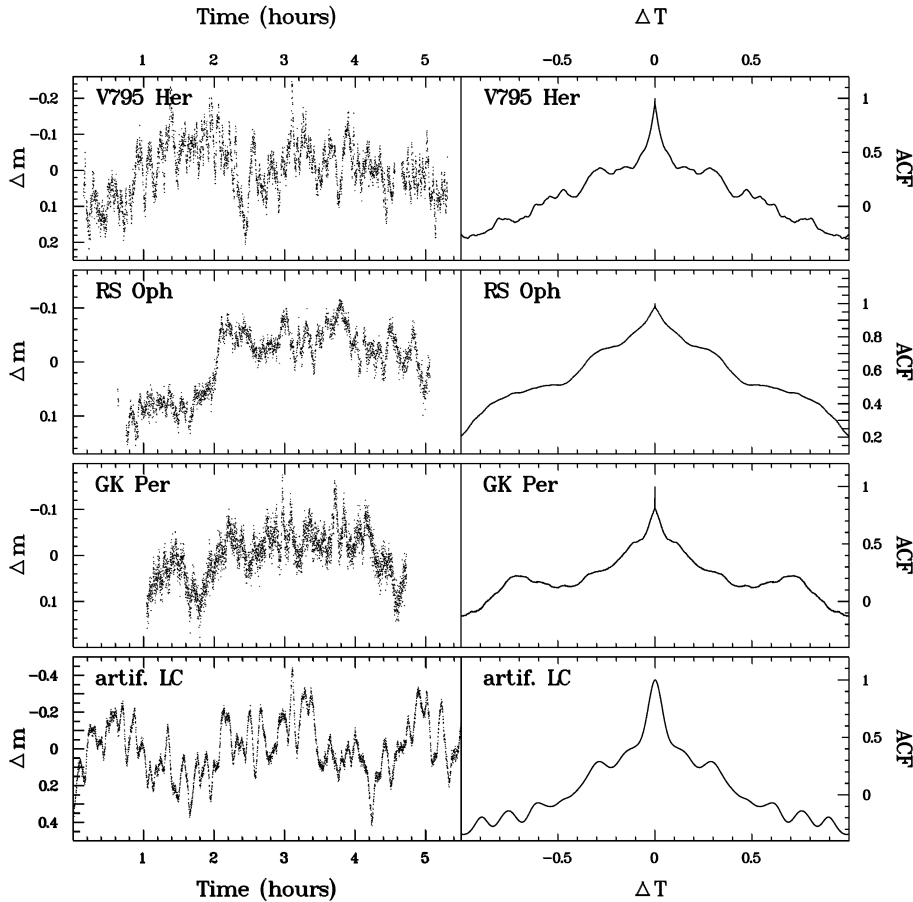


**Fig. 7.** Representative light curves of three cataclysmic variables and an artificial flickering curve (left hand frames) together with their respective auto-correlation-functions (right hand frames).

UX UMa as well as in Z Cha (Bruch 1996) and V893 Sco (Bruch et al. 2000) hot spot flickering is not negligible. In IP Peg this contribution even dominates the flickering while the white dwarf flickering is all but absent.

Let us assume that at phases away from the orbital hump only the white dwarf flickering (which may be termed  $\sigma_{WD}$ ) is visible in the scatter curves. Around hump maximum both, white dwarf flickering and hot spot flickering (termed  $\sigma_{HS}$ ), are superposed. Assuming both contributions to be independent the scatter at hump maximum is then  $\sqrt{\sigma_{HS}^2 + \sigma_{WD}^2}$ . Determining the average of the scatter in the corresponding curves at phases away from the hump and around hump maximum then permits to calculate the ratio  $\sigma_{HS}/\sigma_{WD}$ . Similarly, the mean system brightness during out-of-hump phases,  $F_{ooh}$ , is due to all light sources except the hot spot, while during hump maximum it is the sum of the hot spot brightness,  $F_{HS}$ , and  $F_{ooh}$ . Measuring the brightness levels in the mean light curves (no calibration is required because only ratios are of interest here) during the respective phase intervals yields the ratio  $F_{HS}/F_{ooh}$ , i.e. the hot spot flux relative to the flux due to all other light sources of the system. In Fig. 8,  $\sigma_{HS}/\sigma_{WD}$  is plotted as a function of  $F_{HS}/F_{ooh}$  for the stars investigated in this study as well as for Z Cha and V893 Sco. The data for the latter two stars were taken from Bruch (1996) and Bruch et al. (2000), respectively.

Not unexpectedly, Fig. 8 suggests a general rise of the relative contribution of the hot spot flickering with increasing am-

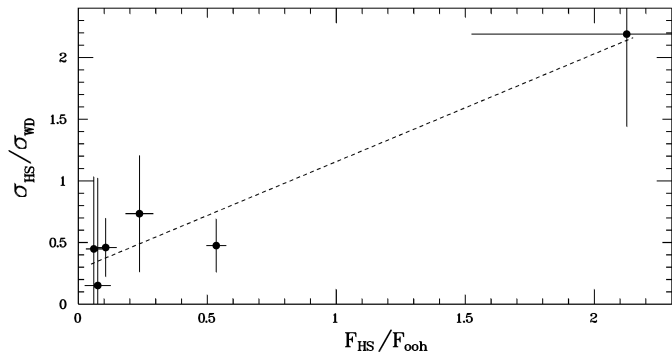


**Fig. 8.** Ratio of the scatter due to hot spot and white dwarf flickering as a function of the brightness ratio of the hot spot and other light sources in six CVs.

plitude of the orbital hump. However, the scatter of the data points is substantial, emphasizing the peculiar behaviour of the individual CVs. Therefore, the formal linear least squares fit, shown as a dashed line in Fig. 8, should only be regarded as an approximate representation of the increase of the relative hot spot flickering strength with the hump amplitude. This is the more so since it obviously depends heavily on the point in the upper right corner which corresponds to IP Peg.

Warner & Nather (1971) first stated that the hot spot flickering might be due to unsteady mass transfer from the secondary

star. The question as to why it is unsteady has not yet been addressed and will also not be discussed in more detail here. I content myself in speculating that variations in the upper atmosphere of the red dwarf may cause more or less material to pass through the  $L_1$  point. Oscillations similar in nature to solar oscillations, occurring on time scales of minutes, might be responsible. Alternatively (as the referee pointed out) shocks and turbulences could be generated by the impact of the transferred matter on the accretion disk and thus cause flickering even if the mass transfer rate is constant.

Concerning the white dwarf flickering the situation is similar. It has been presumed by Bruch (1992) that unsteady accretion out of the inner disk onto the white dwarf surface could be responsible. However, it is unclear which physical mechanism might cause such instabilities. Lyubarskii (1997) has outlined a scenario of how small scale disk instabilities could possibly cause flickering. It is planned to pursue these ideas further in order to verify if they can lead to an explanation for the white dwarf flickering.

*Acknowledgements.* I am deeply indebted to Drs. R.E. Nather, D. O'Donoghue, E.L. Robinson and B. Warner who gave me access to their data archives. Without their support this study could have not been performed. I am also grateful to an anonymous referee for an extraordinarily helpful and considerate report. This work was supported by grants of the Conselho Nacional de Desenvolvimento Científico e Tecnológico (No. 301784/95-5) and the Deutsche Forschungsgemeinschaft (No. Br. 706/8-1/8-2).

## References

Augusteijn T., Karatasos K., Papadakis G., et al., 1992, *A&A* 265, 177  
 Baptista R., Horne K., Hilditch R.W., Mason K.O., Drew J.E., 1995, *ApJ* 448, 395  
 Baptista R., Catalán M.S., Horne K., Zilli D., 1998, *MNRAS* 300, 233

Bennie P.J., Hilditch R.W., Horne K., 1996, in: Evans A., Wood J.H. (eds.), *Cataclysmic Variables and Related Objects*, Proc. IAU Coll. 158, Dordrecht: Kluwer, p. 33  
 Bruch A., 1992, *A&A* 266, 237  
 Bruch A., 1996, *A&A* 312, 97  
 Bruch A., Steiner J.E., Gneiding C., 2000, *PASP* 112, 237  
 Dobrzycka D., Kenyon S.J., Milone A.A.E., 1996, *AJ* 111, 414  
 Echevarría J., Alvarez M., 1993, *A&A* 275, 187  
 Fritz T., Bruch A., 1998, *A&A* 332, 586  
 Herbst W., Shevchenko K.S., 1999, *AJ* 118, 1043  
 Herbst W., Herbst D.K., Grossman E.J., Weinstein D., 1994, *AJ* 108, 1906  
 Hiltner W.A., Mook D.E., 1967, *ApJ* 150, 851  
 Horne K., Stiening R.F., 1985, *MNRAS* 216, 933  
 Horne K., Wood J.H., Stiening R.F., 1991, *ApJ* 378, 271  
 Lyubarskii Yu.E., 1997, *MNRAS* 292, 679  
 Patterson J., 1981, *ApJS* 45, 517  
 Robinson E.L., Warner B., 1972, *MNRAS* 157, 85  
 Sandage A., Westphal J.A., Kristian J., 1969, *ApJ* 156, 927  
 Warner B., Cropper M., 1983, *MNRAS* 203, 909  
 Warner B., Nather R.E., 1971, *MNRAS* 152, 219  
 Warner B., O'Donoghue D., 1987, *MNRAS* 224, 733  
 Welsh W.F., Wood J.H., 1995, in: Greiner J., Duerbeck H.W., Gershberg R.E. (eds.), *Flares and Flashes*, Proc. IAU Coll. 151, Heidelberg: Springer, p.300  
 Welsh W.F., Wood J.H., Horne K., 1996, in: Evans A., Wood J.H. (eds.), *Cataclysmic Variables and Related Objects*, Proc. IAU Coll. 158, Dordrecht: Kluwer, p.33  
 Wolf S., Mantel K.H., Horne K., Barwig H., Schoembs R., Baernbantner O., 1993, *A&A* 273, 160  
 Wood J.H., Horne K., Berriman G., Wade R.A., O'Donoghue D., Warner B., 1986, *MNRAS* 219, 629  
 Wood J.H., Horne K., Berriman G., Wade R.A., 1989a, *ApJ* 341, 974  
 Wood J.H., Marsh T.R., Robinson E.L., et al., 1989b, *MNRAS* 239, 809  
 Zhang E.-H., Robinson E.L., Nather R.E., 1986, *ApJ* 305, 740